Calcif Tissue Int (2010) 87:246–253
DOI 10.1007/s00223-010-9385-9

Effects of P-Glycoprotein on Steroid-Induced Osteonecrosis of the Femoral Head

Ning Han · Zuoqin Yan · Chang-an Guo · Feng Shen · Jun Liu · Yuxing Shi · Zhiyong Zhang

Received: 27 August 2009 / Accepted: 23 May 2010 / Published online: 1 July 2010

Abstract P-glycoprotein (P-gp) activity may play an important role in steroid-induced osteonecrosis of the femoral head (ONF); however, the precise mechanism of its pathogenesis remains unknown. Therefore, we investigated the effects of increased P-gp activity on steroid-induced ONF using a rat model. Rats ($n = 60$) were treated with either a pharmacological stimulant of P-gp, rifampicin (group A); a suppressant, verapamil (group B); or normal saline (group C) administered in conjunction with methylprednisolone, an inducer of ONF. P-gp activity in bone marrow cells and expression in the femoral head significantly increased in group A ($P < 0.05$) but decreased in group B ($P < 0.05$). Likewise, the serum osteocalcin level, trabecular thickness and number, osteoclast and osteoblast numbers, and mean percentage of the epiphyseal ossification center were significantly increased in group A ($P < 0.01$) but decreased in group B ($P < 0.01$). In contrast, however, adipocytic variables, trabecular separation, and apoptotic cells decreased in group A ($P < 0.01$) but increased in group B ($P < 0.01$). The ONF incidence in group A (50%) and group B (100%) was significantly different from that in the control group C (80%, $P < 0.05$). Taken together, our findings suggested that enhanced P-gp activity was able to decrease the risk of steroid-induced ONF, possibly by inhibiting adipogenesis and apoptosis in the femoral head.

Keywords P-glycoprotein · Steroid · Osteonecrosis · Bone marrow stromal cell · Adipogenesis

Osteonecrosis of the femoral head (ONF) is one of the most serious complications induced by high dosages and/or long-term administration of steroid hormones [1–3]. Unfortunately, the underlying pathomechanism of ONF has not yet been elucidated. Progression of steroid-induced ONF often leads to femoral head collapse, resulting in severe hip pain and impaired hip joint function; indeed, most cases of ONF eventually require surgical intervention such as osteotomy, fibula bone graft, or total hip arthroplasty. Focused efforts toward the absolute prevention of ONF onset are crucial.

Recent studies have found that P-glycoprotein (P-gp), a member of the ATP-binding cassette transporter superfamily, is related to the development of steroid-induced ONF. In particular, increased P-gp activity was found to be a statistically relevant marker for low risk of developing steroid-induced ONF [2, 3]. P-gp was initially characterized by its association with the onset of multidrug resistance in chemotherapy patients [4]. Subsequent studies into its function and expression profile have revealed that P-gp plays an important role in the disposition and pharmacological activity of a broad range of therapeutic compounds throughout normal tissues in the mammalian body.

The common pharmacological agents rifampicin and verapamil have been identified, respectively, as an inducer

The authors have stated that they have no conflict of interest.

N. Han · Z. Yan (✉) · C. Guo · F. Shen · J. Liu
Zhongshan Hospital of Fudan University, 180 Fenglin Road, Shanghai 200032, China
e-mail: yan.zuoqin@zs-hospital.sh.cn

Z. Yan
Shanghai Medical College of Fudan University, Shanghai, China

Y. Shi · Z. Zhang
Public Health Clinical Center Affiliated to Fudan University, Shanghai, China

and an inhibitor of P-gp activity in tumor cells [5–8]. Since bone marrow stromal cell (BMSC) adipogenesis is a principal mechanism involved in the onset and progression of steroid-induced ONF [9–11], we carried out preliminary investigations into the effects of rifampicin and verapamil treatment in BMSCs isolated from Sprague-Dawley rats; our findings revealed a similar modification pattern for P-gp activity. We then aimed, in this study, to further investigate the in vivo effects of P-gp activity on steroid-induced osteonecrosis, as enhanced by rifampicin or inhibited by verapamil. Other studies have shown that enhanced P-gp activity is capable of decreasing the intracellular availability of glucocorticoids [3, 4] and that glucocorticoid hormones are well-established contributors to ONF [12]. Since glucocorticoids are known substrates of P-gp, we hypothesized and tested whether P-gp is able to prevent glucocorticoid-induced adipogenesis or apoptosis.

Materials and Methods

Animals

The experimental protocol was carried out as approved by the local Ethical Committee of Animal Experimentation of Fudan University. Sixty male Sprague-Dawley rats (body weight 250–300 g, 7 weeks old) were raised under controlled temperature (24 ± 2°C) and humidity (55 ± 2%) at the Public Health Clinical Center Affiliated with Fudan University. Rats were randomly divided into three groups, group A ($n = 20$), group B ($n = 20$), and group C ($n = 20$), which received daily oral rifampicin (Sigma, St. Louis, MO; 10 mg/kg/day), intraperitoneal verapamil (Sigma, 25 mg/kg/day), or oral saline (2 mL), respectively, for 5 weeks. All groups also received subcutaneous injections of the glucocorticoid methylprednisolone sodium succinate (MPSL; Pfizer Manufacturing, Puurs, Belgium; 21 mg/kg/day) from the second week onward. All rats were killed by anesthesia overdose at the end of the fifth week. Blood samples were collected via intracardiac aspiration. Bone marrow cells were harvested by flushing from the femoral shafts with complete Dulbecco's modification of Eagle medium (DMEM; GIBCO, Gaithersburg, MD) containing 10% fetal bovine serum (Biochemical Industries, Beth-Haemek, Israel). The right proximal femurs were fixed in paraformaldehyde for 48 h and decalcified with 10% EDTA (Sigma) solution for 3 weeks; then, bones were cut along the axis of the femoral neck and through the teres ligament for subsequent macropathological analysis. Four-micrometer sections were used for immunohistology and histology. The left femoral heads were used for Western blot analysis.

Serum Osteocalcin Analysis

Serum was separated from 2-mL blood samples. Osteocalcin (OC) was measured using an ELISA kit (Biomedical Technologies, Staughton, IN) specific for rat OC. The concentration of the reaction product was determined from a standard curve.

P-gp Activity Assay in Bone Marrow Cells

P-gp activity was detected as described by Feller et al. [13]. Since rhodamine123 is passively transported into the cells and can be pumped out by P-gp, enhanced P-gp activity would be expected to decrease the overall intracellular rhodamine123 fluorescence. Thus, the retention of intracellular fluorescence was used to indirectly measure P-gp activity, wherein P-gp activity increased as the mean fluorescent value decreased. Bone marrow cells were disrupted mechanically and suspended in phosphate-buffered saline (PBS). The cells were carefully poured over a percoll gradient (d = 1.073 g/mL, Sigma) and centrifuged at $900\times g$ for 20 min. The intermediate zone, enriched with BMSCs, was diluted with an equal volume of PBS and centrifuged at $900\times g$ for 10 min. The resulting pellet was resuspended in complete DMEM supplemented with 2 μg/mL rhodamine123 and maintained in a humidified atmosphere of 5% CO_2 at 37°C for 10 min, then again centrifuged at $200\times g$ for 10 min and washed twice with PBS containing 10% fetal bovine serum. Next, samples were incubated in DMEM containing 10% fetal bovine serum in a humidified atmosphere of 5% CO_2 at 37°C for 60 min and immediately analyzed by flow cytometry (FCM; BD Biosciences, Franklin Lakes, NJ). Excitation and emission wavelengths used were 488 and 525 nm for rhodamine123, respectively. Samples (50 μL) without rhodamine123 were analyzed by FCM as controls.

Immunohistochemical Staining for P-gp in the Femoral Head

After deparaffinization and rehydration, sections were treated with 0.5% hydrogen peroxide to block endogenous peroxidase activity, followed by incubation with normal rabbit serum (Dako, Hamburg, Germany) for 30 min at 37°C. Then, primary anti-P-gp monoclonal antibody C219 (1:20 dilution; Abcam, Cambridge, UK) was added and samples were incubated overnight at 4°C. The next morning, tissue sections were incubated with a secondary rabbit anti-mouse antibody (Dako) and with horseradish peroxidase (HRP)–labeled streptavidin (Dako). The final reaction product was revealed by exposure to 0.03% diaminobenzidine (DAB, Sigma). Nuclei were counterstained

with hematoxylin. For each specimen, a negative control was obtained by omitting the primary antibody.

Western Blot to Detect P-gp Expression in the Femoral Head

The left femoral heads were snap-frozen in liquid nitrogen, crushed in RIPA buffer with a tissue grinder, and extracted by incubation at 4°C for 30 min. The lysates from each were subsequently centrifuged at 15,000×*g* at 4°C for 10 min. The protein concentrations of soluble fractions were measured with BCA protein assay reagent (Pierce, Rockford, IL). Laemmli buffer (6×) was added to each sample to a final concentration of 1× , and 50 μg of each preparation was loaded onto 10% SDS polyacrylamide gels. After electrophoresis, proteins were transferred onto nitrocellulose membranes (Schleicher & Schuell, Dassel, Germany) and immunolabeled with C219 (1:20) overnight at 4°C. HRP-labeled goat anti-mouse (Santa Cruz Biotechnology, Santa Cruz, CA) was used as a secondary antibody. Proteins were detected with an enhanced chemiluminescence kit (Amersham Life Sciences, Arlington Heights, IL), after which the membranes were exposed to autoradiographic films for 20 min (Eastman Kodak, Rochester, NY). Relative expressions were quantified densitometrically using Quantity One software (Bio-Rad, Richmond, CA) and calculated by normalization to the reference bands of β-actin.

Histological Examination

Macropathological findings were observed by stereomicroscopy. Using Image Pro Plus 6.0 software (Media Cybernetics, Silver Spring, MD), the proportion of the ossification center in the epiphysis was calculated by the area of the ossification center divided by the area of the epiphysis.

Sections were stained with hematoxylin and eosin (H-E). Microphotos were captured from each slice of every femoral head sample under ×40 magnification. Image Proplus 6.0 software was used to determine the three-dimensional (3D) structural parameters of trabeculae, including trabecular thickness (Tb.Th), trabecular number (Tb.N), and trabecular separation (Tb.Sp), using 2D measurements of bone perimeter, bone area, and tissue area, according to Parfitt's plate model for cancellous bone structure [14, 15]. Meanwhile, adipogenesis was assessed by determining the adipose tissue area, number of adipocytes (N.At/M.Ar), and adipocyte perimeter. The adipose tissue area was expressed as the percentage of the total bone marrow area occupied by adipocytes. The number of adipocytes was expressed as the total adipocytes per bone marrow area; the adipocyte perimeter was expressed in microns.

Alkaline phosphatase staining and tartrate-resistant acid phosphatase (TRAP) staining were used to identify osteoblasts and osteoclasts. The following primary parameters were determined at ×200 magnification: osteoclast numbers (N.Oc/B.Pm) and osteoblast number (N.Ob/B.Pm); each were expressed using the bone perimeter (B.Pm) as a reference. Osteoclast perimeter (Oc.Pm/B.Pm) was expressed using the bone perimeter as a reference.

According to the criteria of Ficat [16] and Murata et al. [1], we defined early osteonecrosis as a condition in which the marrow cells had disappeared or had degenerated and bone marrow spaces had been filled with adipocytes, though trabecular osteocytes were still alive. Based on the histological findings, the incidence of ONF was designated as the rate of osteonecrosis observed in the 40 femoral heads.

TUNEL Staining

Using the In Situ Cell Death Detection Kit, Fluorescein (Roche Applied Science, Indianapolis, IN), we performed a TUNEL assay according to the manufacturer's instructions. Apoptotic cells presented green fluorescence under fluorescence microscopy. Five microphotos of areas containing significant apoptosis were captured from each slice of every femoral head sample at ×200 magnification. TUNEL-positive cells were counted in the photos.

Statistical Analysis

All data, except the incidence of ONF, were expressed as the mean ± standard deviation (SD) and analyzed by the *t*-test using the STATA statistical software package (version 7.0; StataCorp, College Station, TX). The incidence of ONF was analyzed by the chi-squared test. $P < 0.05$ was considered to be statistically significant.

Results

OC Levels Are Modified by Exposure to P-gp Inducer and Inhibitor

The OC level in rifampicin P-gp inducer–treated rats (group A, 17.26 ± 3.95) was the highest observed for all the groups ($P < 0.01$). Likewise, the OC level in verapamil P-gp inhibtor–treated rats (group B, 11.78 ± 1.47) was lower than that in controls (group C, 15.02 ± 2.13; $P < 0.01$).

P-gp Activity in Bone Marrow Cells

In the bone marrow cells of P-gp modulator–treated rats, the mean fluorescent value in the enhanced group A was

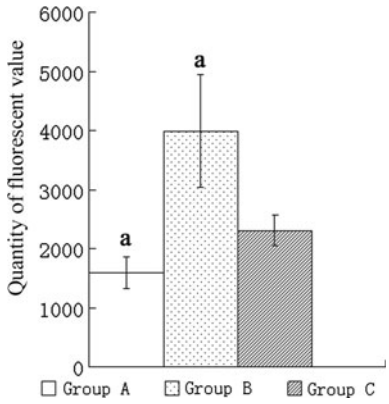

Fig. 1 P-gp activity in bone marrow cells. The quantity of intracellular fluorescent value represents P-gp activity; the value is inversely proportional to P-gp activity: lower intracellular fluorescence indicates enhanced P-gp activity. P-gp activity was enhanced by rifampicin (group A) and inhibited by verapamil (group B) compared with group C. Results are expressed as mean ± SD. $^{a}P < 0.01$ relative to group C

the lowest for all the groups, indicating that P-gp activity was increased and able to actively pump out the intracellular fluorescence protein. Likewise, the mean fluorescent value in the P-gp-inhibited group B was higher than that in group C ($P < 0.01$) (Fig. 1).

P-gp Expression in the Femoral Head

Positive immunohistochemical staining was apparent in many bone marrow cells, most of which were identified as hemopoietic cells, and a few in osteocytes and osteoblasts (Fig. 2a).

According to quantification by Western blot analysis, the P-gp expression in the femoral heads of the P-gp-enhanced group A was the highest of all three groups ($P < 0.01$). P-gp expression in inhibited group B was lower than that in control group C (Fig. 2b, c).

P-gp Activity Decreases the Histological Signs of ONF

Based on gross observation, the epiphyseal ossification center was observed to be smaller and the cartilage thicker in P-gp-inhibited group B compared with the other groups (Fig. 3a). The mean percentage of the epiphyseal ossification center in the femoral head epiphysis in P-gp-enhanced group A was the largest ($P < 0.01$), while the mean percentage of group B was significantly smaller than that of group C ($P < 0.01$) (Table 1).

Tb.Th and Tb.N were determined to be the highest and the Tb.Sp the lowest in response to P-gp enhancement (group A, $P < 0.01$). In response to P-gp inhibition, Tb.Th and Tb.N were significantly decreased and Tb.Sp was significantly increased over the values measured in controls (group C) (Fig. 3b, Table 1). The adipose tissue area and the number and presence of perimeter adipocytes in group A were significantly lower compared with the other two groups ($P < 0.01$); not surprisingly, these parameters were higher in group B than in group C ($P < 0.01$) (Figs. 3b, 4). N.Oc/B.Pm, Oc.Pm/B.Pm, and N.Ob/B.Pm were the most increased by P-gp inducer exposure (group A, $P < 0.01$), whereas they were significantly lower in group B than in group C (Table 1).

By histological analyses, osteonecrosis was observed in 10 of 20 samples in group A (50%), 20 of 20 samples in

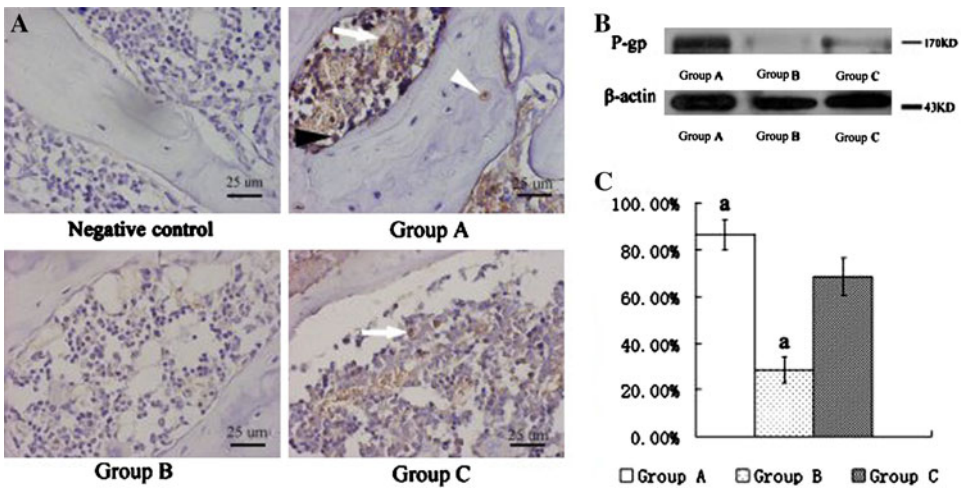

Fig. 2 P-gp expression in the femoral head. P-gp expression in the femoral head was enhanced by rifampicin (group A) and inhibited by verapamil (group B) in comparison with group C. **a** Immunohistochemical staining for P-gp in the femoral head. Positive staining mainly appeared in bone marrow cells (*white arrow*), a few osteocytes (*white arrowhead*), and osteoblastic cells (*black arrowhead*). **b** Western blot. **c** The amount of P-gp was measured by densitometry and normalized to that of β-actin. Results are expressed as mean ± SD. $^{a}P < 0.01$ relative to group C

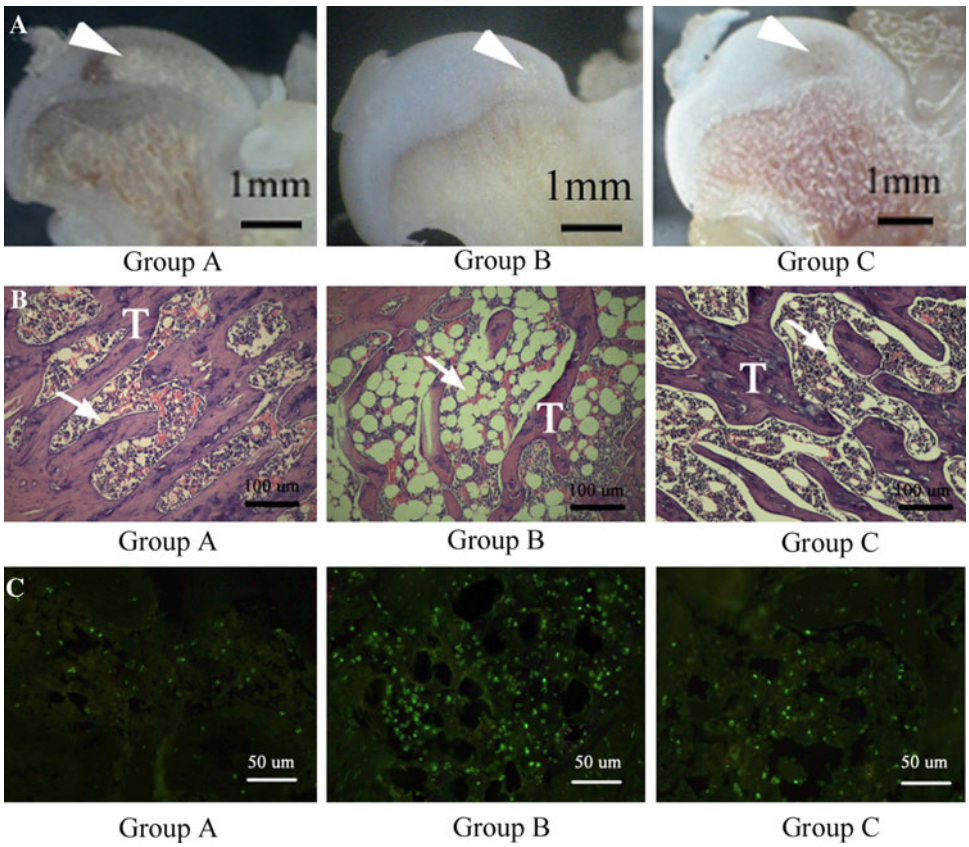

Fig. 3 Coronal sections through the teres ligament of the femoral head. **a** Macropathology. With the same dose of MPSL, the size of the EOC (*white arrowhead*) increased in response to rifampicin (group A) and decreased in response to verapamil (group B) compared with group C. **b** H-E staining. With the same dose of MPSL, the number and thickness of trabeculae (*T*) increased in response to rifampicin (group A) and decreased in response to verapamil (group B) compared with group C. The separation of trabeculae as well as the size and number of adipocytes (*white arrow*) decreased in response to rifampicin (group A) and increased in response to verapamil (group B) compared with group C. **c** TUNEL staining. With the same dose of MPSL, the number of apoptotic cells (*green fluorescence*) decreased in response to rifampicin (group A) and increased in response to verapamil (group B) compared with group C

group B (100%), and 16 of 20 samples in group C (80%). There was a significant difference of the incidence of ONF among the three groups ($P < 0.05$). These findings indicated that P-gp activity correlated with a decreased risk of developing ONF in our animal model.

P-gp Activity Is Associated with Decreased Apoptosis

In group A, the number of apoptotic cells was significantly lower than that observed in group C ($P < 0.01$). In contrast, inhibition of P-gp activity (in group B) led to the presence of significant amounts of apoptotic cells ($P < 0.01$) (Fig. 3c, Table 1).

Discussion

In the present study, P-gp activity was effectively enhanced by rifampicin treatment and decreased by verapamil. As a result, the incidence of steroid-induced ONF was successfully decreased by rifampicin and increased by verapamil. To the best of our knowledge, this is the first study to investigate the effects of P-gp activity on steroid-induced ONF using a P-gp inducer and inhibitor.

Steroid-induced ONF is generally considered to have a multifactorial pathogenesis, in which adipogenesis of BMSC is a principal pathological mechanism. An earlier study by Cui et al. [17] indicated that BMSCs, even with primarily osteogenic properties, became adipogenic in response to MPSL in vivo. Fatty marrow is a well-established early histological manifestation of ONF in vivo [1, 16]. The results from our study using a rat glucocorticoid-induced ONF model also demonstrated that there was massive adipocyte proliferation in the marrow space in the control group. P-gp activity has been shown to modulate intracellular concentration of glucocorticoids [5, 18–20], and higher concentrations of glucocorticoids enhanced BMSC adipogenesis in vitro and in vivo [21–24]. In this study, when rifampicin and verapamil were administered in conjunction with ONF-inducing steroids, the P-gp activity

Table 1 Effects of P-gp on steroid-induced ONF as assessed by histomorphometry

	Group A	Group B	Group C
EOC (%)	39.02 ± 2.42*	11.84 ± 2.65**	26.96 ± 9.63
Tb.Th (μm)	55.65 ± 7.14*	44.06 ± 2.86 **	52.63 ± 8.54
Tb.N (N/mm)	9.24 ± 1.72*	5.92 ± 1.55**	8.19 ± 2.81
Tb.Sp (μm)	111.26 ± 20.65*	179.29 ± 44.91**	138.35 ± 53.29
Apoptosis	38.87 ± 18.91*	123.56 ± 27.86**	87.26 ± 19.33
N.Oc/B.Pm (*n*/mm)	2.74 ± 1.23*	1.08 ± 1.04**	1.96 ± 1.07
Oc.Pm/B.Pm (%)	0.70 ± 0.31*	0.31 ± 0.21**	0.49 ± 0.26
N.Ob/B.Pm (*n*/mm)	33.40 ± 5.07*	11.11 ± 2.14**	21.66 ± 4.34

EOC epiphyseal ossification center

Quantification of apoptosis expressed as the number of apoptotic cells in the ×200 field. Data expressed as mean ± SD

* $P < 0.01$ relative to groups B and C, ** $P < 0.01$ relative to group C

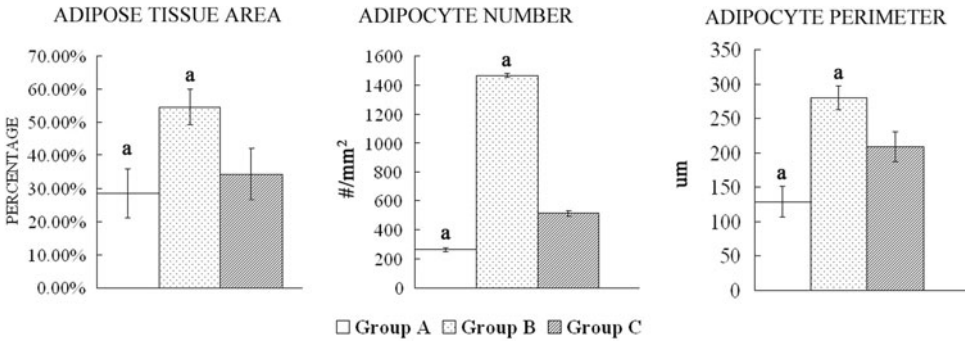

Fig. 4 Adipogenic parameters in the femoral head. **a** Adipose tissue area. **b** Adipocyte number. **c** Adipocyte perimeter. In group A, rifampicin decreased these variables compared with group C. In group B, verapamil increased these variables compared with group C. [a] $P < 0.01$ relative to group C

of bone marrow cells was promoted and inhibited, respectively; more importantly, the number and size of adipocytes and the area of adipose tissue increased when P-gp activity decreased. In contrast, all the adipocytic parameters decreased in response to the P-gp inducer. These findings collectively suggest that the intracellular concentration of MPSL plays an important role in the observed histological changes. Several previous studies have confirmed that the increased amount of bone marrow fat cells within the femoral head was related to a higher incidence of ONF, which may act by elevating intraosseous pressure and reducing blood flow to the femoral head [21, 25, 26]. As a result, the incidence of ONF in our animal model was successfully decreased and increased by rifampicin and verapamil, respectively.

As the precursor of both adipocytes and osteoblasts, BMSCs display inhibited osteogenesis when adipogenesis is enhanced [10, 11]. Hernigou et al. [27] demonstrated that glucocorticoids were able to decrease the number of BMSCs in the proximal femur, which was insufficient to meet the needs of osteogenesis. Decreased bone formation in response to glucocorticoids has been suggested to suppress bone remodeling in the femoral head, leading to osteonecrosis [27]. Bone remodeling is a perpetual event characterized by sequential cycling of osteoclast and osteoblast activities [28]. In the mammalian system, steroids act directly on osteoblasts and osteoclasts to regulate bone remodeling, which is crucial to repair bone injuries induced by high-level or prolonged glucocorticoid exposure [12, 29]. Maintenance of high concentrations of glucocorticoids was found to decrease the number of osteoblasts and osteoclasts and to cause attenuation of bone formation [28–31]. Likewise, inhibition of P-gp activity has been shown to increase the accumulation and, thus, effect of glucocorticoids in vivo [3, 19, 23]. In our study, when P-gp expression was suppressed by verapamil in group B, the number of osteoblasts and osteoclasts decreased as a result of the accumulation of intracellular MPSL. Serum OC is a sensitive marker of the rate of bone turnover and can be suppressed by glucocorticoids [32, 33]. When P-gp activity and expression were inhibited by verapamil, OC was also found to have decreased significantly; in addition, bone formation and remodeling were inhibited, which eventually led to increased Tb.Sp and decreased Tb.Th and Tb.N.

Furthermore, retardation of normal growth is a serious complication of corticosteroid exposure. This side effect is believed to be a result of the inhibitory effect on ossification, depending on the dose and duration of steroid administration [34]. When P-gp was pharmacologically

inhibited in our study, excessive adipogenesis was found to occur in the femoral head. Moreover, bone formation in the epiphysis was inhibited because of decreased precursors available for osteoblast maturation.

Recently, apoptosis has been reported as another important mechanism underlying steroid-induced ONF [12, 30]. Our findings, presented herein, demonstrated that the apoptosis rate decreased obviously when P-gp expression in the femoral heads was enhanced by rifampicin; we speculate that this effect might be also due to attenuated intracellular availability of MPSL. A higher concentration of glucocorticoids is known to induce more significant apoptosis in osteoblasts, osteocytes, osteoclasts, and peripheral blood mononuclear cells [12, 30, 35, 36]. Our immunostaining analysis demonstrated similar findings; increased apoptosis of osteocytes and osteoblasts disrupted bone remodeling. Decreased trabecular thickness and number were observed in our P-gp-inhibited ONF rats, both pathologies being direct contributors to the eventual femoral head collapse [12].

Adipogenesis of BMSCs and apoptosis are both closely related to onset and progression of steroid-induced ONF [12, 22, 27]; however, their exact roles and interrelationships remain to be defined. Toward this goal, our study established that the modulation of P-gp activity has a direct effect on the adipogenesis of BMSCs and apoptosis simultaneously and that these two mechanisms, either in isolation or in combination, may result in steroid-induced ONF.

In conclusion, P-gp plays an important role in steroid-induced ONF, and P-gp activity enhanced by rifampicin could decrease the risk of steroid-induced ONF, at least partially, by inhibiting adipogenesis and apoptosis in the femoral head.

Acknowledgements This work was supported by the Shanghai Natural Science Foundation (grants 07ZR14023 and 10411962500).

References

1. Murata M, Kumagai K, Miyata N, Osaki M, Shindo H (2007) Osteonecrosis in stroke-prone spontaneously hypertensive rats: effect of glucocorticoid. J Orthop Sci 12:289–295
2. Kuribayashi M, Fujioka M, Takahashi KA, Arai Y, Hirata T, Nakajima S, Yoshimura N, Satomi Y, Nishino H, Kondo K, Fukushima W, Hirota Y, Kubo T (2008) Combination analysis of three polymorphisms for predicting the risk for steroid-induced osteonecrosis of the femoral head. J Orthop Sci 13:297–303
3. Asano T, Takahashi KA, Fujioka M, Inoue S, Okamoto M, Sugioka N, Nishino H, Tanaka T, Hirota Y, Kubo T (2003) ABCB1 C3435T and G2677T/A polymorphism decreased the risk for steroid-induced osteonecrosis of the femoral head after kidney transplantation. Pharmacogenetics 13:675–682
4. Karssen AM, Meijer OC, van der Sandt IC, De Boer AG, De Lange EC, De Kloet ER (2002) The role of the efflux transporter P-glycoprotein in brain penetration of prednisolone. J Endocrinol 175:251–260
5. Fardel O, Lecureur V, Loyer P, Guillouzo A (1995) Rifampicin enhances anticancer drug accumulation and activity in multidrug-resistant cells. Biochem Pharmcol 49:1255–1260
6. Vautier S, Lacomblez L, Chacun H, Picard V, Gimenez F, Farinotti R, Fernandez C (2006) Interactions between the dopamine agonist, bromocriptine and the efflux protein, P-glycoprotein at the blood–brain barrier in the mouse. Eur J Pharm Sci 27:167–174
7. Odening KE, Li W, Rutz R, Laufs S, Fruehauf S, Fishelson Z, Kirschfink M (2009) Enhanced complement resistance in drug-selected P-glycoprotein expressing multi-drug-resistant ovarian carcinoma cells. Clin Exp Immunol 155:239–248
8. Arellano C, Philibert C, Vachoux C, Woodley J, Houin G (2007) The metabolism of midazolam and comparison with other CYP enzyme substrates during intestinal absorption: in vitro studies with rat everted gut sacs. J Pharm Pharm Sci 10:26–36
9. Li X, Cui Q, Kao C, Wang GJ, Balian G (2003) Lovastatin inhibits adipogenic and stimulates osteogenic differentiation by suppressing PPARgamma2 and increasing Cbfa1/Runx2 expression in bone marrow mesenchymal cell cultures. Bone 33:652–659
10. Sekiya I, Larson BL, Vuoristo JT, Cui JG, Prockop DJ (2004) Adipogenic differentiation of human adult stem cells from bone marrow stroma (BMSCs). J Bone Miner Res 19:256–264
11. Lee JS, Lee JS, Roh HL, Kim CH, Jung JS, Suh KT (2006) Alterations in the differentiation ability of mesenchymal stem cells in patients with nontraumatic osteonecrosis of the femoral head: comparative analysis according to the risk factor. J Orthop Res 24:604–609
12. Kerachian MA, Séguin C, Harvey EJ (2009) Glucocorticoids in osteonecrosis of the femoral head: a new understanding of the mechanisms of action. J Steroid Biochem Mol Biol 114:121–128
13. Feller N, Kuiper CM, Lankelma J, Ruhdal JK, Scheper RJ, Pinedo HM, Broxterman HJ (1995) Function detection of MDR1/P170 and MRP/P190-mediated multidrug resistance in tumor cells by flow cytometry. Br J Cancer 72:543–549
14. Parkinson IH, Fazzalari NL (2003) Interrelationships between structural parameters of cancellous bone reveal accelerated structural change at low bone volume. J Bone Miner Res 18:2200–2205
15. Parfitt AM, Drezner MK, Glorieux FH, Kanis JH, Malluche H, Meunier PJ, Ott SM, Recker RR (1997) Bone histomorphometry: standardization of nomenclature, symbols, and units. J Bone Miner Res 2:595–610
16. Ficat RP (1985) Idiopathic bone necrosis of the femoral head. Early diagnosis and treatment. J Bone Joint Surg Br 67:3–9
17. Cui Q, Wang GJ, Balian G (2000) Pluripotential marrow cells produce adipocytes when transplanted into steroid-treated mice. Connect Tissue Res 41:45–56
18. Barnes KM, Dickstein B, Cutler GB, Fojo T, Bates SE (1996) Steroid transport, accumulation, and antagonism of P-glycoprotein in multidrug-resistant cells. Biochemistry 35:4820–4827
19. Miyanishi K, Yamamoto T, Irisa T, Yamashita A, Motomura G, Jingushi S, Iwamoto Y (2006) Effects of cyclosporin A on the development of osteonecrosis in rabbits. Acta Orthop 77:813–819
20. Kralli A, Yamamoto KR (1996) An FK506-sensitive transporter selectively decreases intracellular levels and potency of steroid hormones. J Biol Chem 271:17152–17156
21. Miyanishi K, Yamamoto T, Irisa T, Yamashita A, Jingushi S, Noguchi Y, Iwamoto Y (2002) Bone marrow fat cell enlargement and a rise in intraosseous pressure in steroid-treated rabbits with osteonecrosis. Bone 30:185–190
22. Yin L, Li YB, Wang YS (2006) Dexamethasone-induced adipogenesis in primary marrow stromal cell cultures: mechanism of steroid-induced osteonecrosis. Chin Med J (Engl) 119:581–588

23. Miyanishi K, Yamamoto T, Irisa T, Yamashita A, Motomura G, Jingushi S, Iwamoto Y (2008) Effects of tacrolimus (FK506) on the development of osteonecrosis in a rabbit model. Immunopharmacol Immunotoxicol 30:79–90
24. Cui Q, Wang GJ, Balian G (1997) Steroid-induced adipogenesis in a pluripotential cell line from bone marrow. J Bone Joint Surg Am 79:1054–1063
25. Motomura G, Yamamoto T, Miyanishi K, Yamashita A, Sueishi K, Iwamoto Y (2005) Bone marrow fat-cell enlargement in early steroid-induced osteonecrosis—a histomorphometric study of autopsy cases. Pathol Res Pract 200:807–811
26. Drescher W, Schneider T, Becker C, Hobolth J, Ruther W, Hansen ES, Bünger C (2001) Selective reduction of bone blood flow by short-term treatment with high-dose methylprednisolone: an experimental study in pigs. J Bone Joint Surg Br 83:274–277
27. Hernigou P, Beaujean F, Lambotte JC (1999) Decrease in the mesenchymal stem-cell pool in the proximal femur in corticosteroid-induced osteonecrosis. J Bone Joint Surg Br 81:349–355
28. Kim HJ, Zhao H, Kitaura H, Bhattacharyya S, Brewer JA, Muglia LJ, Ross FP, Teitelbaum SL (2006) Glucocorticoids suppress bone formation via the osteoclast. J Clin Invest 116:2152–2160
29. Sivagurunathan S, Muir MM, Brennan TC, Seale JP, Mason RS (2005) Influence of glucocorticoids on human osteoclast generation and activity. J Bone Miner Res 20:390–398
30. Weinstein RS, Jilka RL, Parfitt AM, Manolagas SC (1998) Inhibition of osteoblastogenesis and promotion of apoptosis of osteoblasts and osteocytes by glucocorticoids: potential mechanisms of the deleterious effects on bone. J Clin Invest 102:274–282
31. O'Brien CA, Jia D, Plotkin LI, Bellido T, Powers CC, Stewart SA, Manolagas SC, Weinstein RS (2004) Glucocorticoids act directly on osteoblasts and osteocytes to induce their apoptosis and reduce bone formation and strength. Endocrinology 145:1835–1841
32. Clemens TL, Tang H, Maeda S, Kesterson RA, Demayo F, Pike JW, Gundberg CM (1997) Analysis of osteocalcin expression in transgenic mice reveals a species difference in vitamin D regulation of mouse and human osteocalcin genes. J Bone Miner Res 12:1570–1576
33. Erben RG, Stangassinger M, Gärtner R (1998) Skeletal effects of low-dose cyclosporin A in aged male rats: lack of relationship to serum testosterone levels. J Bone Miner Res 13:79–87
34. Sheagren JN, Jowsey J, Bird DC, Gurton ME, Jacobs JB (1977) Effect on bone growth of daily versus alternate-day corticosteroid administration: an experimental study. J Lab Clin Med 89:120–130
35. Seki M, Ushiyama C, Seta N, Abe K, Fukazawa T, Asakawa J, Takasaki Y, Hashimoto H (1998) Apoptosis of lymphocytes induced by glucocorticoids and relationship to therapeutic efficacy in patients with systemic lupus erythematosus. Arthritis Rheum 41:823–830
36. Dempster DW, Moonga BS, Stein LS, Horbert WR, Antakly T (1997) Glucocorticoids inhibit bone resorption by isolated rat osteoclasts by enhancing apoptosis. J Endocrinol 154:397–406